Disuse induced by botulinum toxin affects the bone marrow expression profile of bone genes leading to a rapid bone loss.

H. Libouban, M.-A. Le Drévo, Daniel Chappard

J Musculoskelet Neuronal Interact 2013; 13(1):27-36

Original Article

Hylonome

Disuse induced by botulinum toxin affects the bone marrow expression profile of bone genes leading to a rapid bone loss

H. Marchand-Libouban, M.A. Le Drévo, D. Chappard

LUNAM Université, GEROM – LHEA Groupe d'Etudes Remodelage Osseux et bioMatériaux, IRIS-IBS Institut de Biologie en Santé, CHU d'Angers, 49933 ANGERS Cedex, France

Abstract

Objectives: Molecular events occurring in the bone marrow microenvironment of an immobilized mouse limb after Botulinum toxin (BTX) injection haven't been characterized. BTX injection induces a localized disuse in which the tissue events have well been characterized. **Methods:** BTX injection was performed in the right quadriceps; saline injection in the left side was used as control. Mice were sacrificed at 0, 7, 14, 21 and 28 days; tibias were used for microCT analysis; bone marrow from femurs for RT-PCR analysis. **Results:** MicroCT revealed bone loss and microarchitectural damages on the immobilized side as from 7d; cortical area tended to be lower on the immobilized limb at 28d. Gene expression of formation factors was altered as from 7 days post-BTX: *alkaline phosphatase, Tgfβ1, Lrp5, Sfrp2*. *Only Sfrp2* and *Lrp5* were maintained altered until 28d. Expression of Dkk1 increased from 21d and represented a late inhibitor of formation. Gene expression of resorption markers increased as from 7d (*Rankl, Tracp, Il1α, Il1β* and *Il6*) and was maintained until 28d for *Tracp* and *Il6*. **Conclusion:** A localized disuse induces rapid modifications in the bone marrow gene expression leading to bone loss due to an early decrease of formation associated with an increase in resorption.

Keywords: Disuse, Botulinum Toxin, Gene Expression, Bone Remodeling, Bone Resorption

Introduction

In man, one of the most striking findings observed during disuse and other unloading conditions such as bed rest, spinal cord injury, weightlessness... is a rapid and continuous bone loss due to an unbalanced bone turnover[1]. In paraplegic patients, the number of osteoclast cells is increased in bones under the spinal section compared to bones above the lesion[2]. To reproduce a zero g environment in laboratory animals, prolonged localized disuse of the extremity has been repeatedly used by various surgical techniques such as denervation, spinal cord section, tenotomy or arthrodesis[3]. They lead to a permanent immobilization inducing a rapid bone loss. However, in these models, bone loss results from the cumulative effect of disuse and the regional acceleratory phenomenon caused by the surgical trauma[4]. At the present time, nonsurgical methods such as immobilization by casting, tail suspension, bandaging or *Clostridium botulinum* toxin type A (BTX) injection have become more popular[3,5]. BTX is a bacterial metalloprotease that acts in the cytosol of cholinergic nerve terminals. It degrades cytosolic core proteins of the neuroexocytosis apparatus causing an inhibition of the neurotransmitter release[6]. Such inhibition is fully reversible in several months, following the degradation of the internalized toxin and re-synthesis of the cleaved proteins[7]. We have previously developed the disuse model due to BTX injection in the rat and reported a significant bone loss on the proximal tibia and on the distal femur from the immobilized hindlimb after 1 month[5]. Moreover, combination of BTX injection and orchidectomy induces a more severe bone loss than orchidectomy alone[8]. The model was also adapted in mice by others[9-11]. Most of the studies done with the BTX model have focused on tissue data and, at that time, no investigation has been done to explain the mechanisms implicated in bone loss. The local expression of several genes implicated in bone remodeling can be assessed to specify the mechanisms of bone loss. Bone marrow microenvironment includes mostly non-adherent cells of hematopoietic origin and

The authors have no conflict of interest.

Corresponding author: Hélène Marchand-Libouban, Ph.D., GEROM-LHEA, IRIS-IBS Institut de Biologie en Santé, LUNAM Université, CHU d'Angers, 49933 ANGERS Cedex, France
E-mail: helene.marchand-libouban@univ-angers.fr

Edited by: M. Hamrick
Accepted 14 February 2013

a small proportion of adherent cells, comprising mesenchymal stem cells (MSCs). Different intracellular and extracellular signals control differentiation of MSCs into osteoblasts. The *Runx2* (runt-related transcription factor-2; previously known as Core-binding factor α1 - *Cbfa1*), is a transcription factor of the *Runt* domain gene family identified as an essential transcriptional activator of osteoblast differentiation and represents a master gene for bone[12]. Osteoblasts also express high levels of alkaline phosphatase activity (ALP) which contributes to bone mineralization[13]. More recently, the Wnt pathway has been found to play a key role for osteoblast maturation and bone formation[14]. Loss of function in *Lrp5* leads to an extremely low bone mass phenotype[15]. Several antagonist molecules (sFRP2, DKK1, Sclerostin) of the Wnt pathway have a physiological role in the negative control of bone formation. Osteoblasts regulate recruitment and activity of osteoclasts through the expression of receptor activator of NF-ϰB ligand (RANKL) and osteoprotegerin (OPG) and the RANK/RANKL/OPG system has a key role in bone resorption[16,17]. The aim of the present study was to elucidate the molecular events that occur in the bone marrow microenvironment during bone loss due to a localized disuse induced by a single BTX injection. Bone loss was controlled in parallel by X-ray micro computed tomography (microCT) on the tibias.

Material and methods

Animals

Forty female Swiss mice (Harlan, France), aged 10 weeks and weighing 27.9±2.0 g were acclimated for 1 week under conventional conditions (24°C and a 12h/12h light/dark cycle) in the animal house facility of the University of Angers, France (Agreement A 49 007 002). *In vivo* experiments were performed in accordance with the regulations of the official edict of the French Ministry of Agriculture, under the supervision of authorized researchers (autorization # 49028).

Mice were given a standard laboratory food (UAR, Villemoison sur Orge, France) and water *ad libitum*. Mice were randomly spread into 5 groups of 8 mice each. At day 0, mice from 4 groups were weighted, anesthetized with isoflurane and injected intramuscularly with 0.5 U of BTX (Allergan®, France) in the right muscle *quadriceps femoris*. This injected side will be referred as the immobilized limb (I); an injection with a same volume of saline was done in the left hindlimb which will be referred as the non-immobilized limb (NI) and will serve as control. Mice were weighted and sacrificed at 7, 14, 21 and 28 days by cervical dislocation. The remaining eight mice were not injected; they were sacrificed at day 0 and constituted the baseline group (B). For all mice, tibia and femur were dissected and defleshed. The tibias were used for X-ray micro computed tomography; the femurs were then used for real-time quantitative RT-PCR analysis.

X-ray micro computed tomography

MicroCT was performed on the proximal tibia extremity with a Skyscan 1072 microtomograph (Bruker MicroCT, Skyscan, Kontich, Belgium) equipped with an X-ray tube working at 80 kV and 100 μA. each tibia was placed in an Eppendorf's tube and filled with water to prevent desiccation. The tube was fixed on a brass stub with plasticine and analyzed with a pixel size corresponding to 5.25 μm, the rotation step was fixed at 0.45°, and exposure was done with a 0.5 mm aluminum filter. For each tibia, a stack of 2D-sections was obtained. The CTAn Software (Skyscan, release 2.5) was used for measuring the bone mass and microarchitecture at the secondary spongiosa of the tibia. The upper limit of the volume of interest was located just after the disappearance of the growth plate and primary spongiosa; the lower limit was located 200 sections below. A threshold was determined interactively to eliminate background noise and to select bone. The volume of interest (VOI) was designed by drawing interactively polygons on the 2D sections. Only a few number of polygons needs to be drawn (e.g. starting, some at the middle, and on the final section) since a routine facility calculated all the intermediary masks by interpolation. The VOI comprised only trabecular bone and the marrow cavity. The following parameters were measured according to the recommendations of the American Society for Bone and Mineral Research[18]. Trabecular bone volume (BV/TV, in %) represents the percentage of the cancellous space occupied by trabecular bone in the VOI, Trabecular thickness (Tb.Th, in μm), trabecular separation (Tb.Sp, in μm), and trabecular number (Tb.N, in 1/mm) provide a full description of bone microarchitecture. Structure model index (SMI) indicates the composition of trabecular bone in the form of rods or plates. SMI values are comprised between zero (ideal plate structure model) and three (ideal rod structure). The 3D models were obtained from the stack of 2D images with a surface-rendering program (Ant, release 2.0.5, Skyscan, Belgium).

Measurements on cortical bone were performed using ImageJ 1.45 software on 2D sections of the tibia at the diaphyseal shaft (3.14 mm under the growth cartilage). Several parameters were measured: cortical thickness (Ct.Th, mm), cortical area (Ct.Ar, mm^2), area within the periosteal envelope (Ps.Ar, mm^2), area within the endosteal envelope (Es.Ar, mm^2) and cortical porosity (%).

Real-time quantitative RT-PCR

Bone marrow from each femur was flushed in 200 μl of RNAlater® (Applied Biosystems, Courtaboeuf, France) and stored at -80°C until processing. Total RNA were extracted using trizol/chloroforme extraction followed by RNeasy mini kit (Qiagen, Courtaboeuf, France) according to the manufacturer's procedure; they were then stored at -80°C until use. The quality and concentrations of the RNA were examined on Experion automated electrophoresis system (BioRad, Courtaboeuf, France).

Reverse-transcription

One μg of total RNA was mixed with 3 μg of random hexamers (Invitrogen, Cergy Pontoise, France) in 10 μl final volume, incubated at 70°C for 5 min and chilled on ice. Then the reaction was performed at 25°C for 10 min, 42°C for 1h and 70°C for 10 min with 10 mM of deoxynucleotide triphosphate,

Gene	Forward	Reverse
Runx2	GTGGCCACTTACCAC AGAGC	GTTCTGAGGCGGGACACC
Alp	TGCCAGAGAAAGAGAGAGACC	CAGCGGTTACTGTGGAGACG
Tgfβ1	CACCATCCATGACATGAACC	CAGAAGTTGGCATGGTAGCC
Lrp5	GGTCACCTGGACTTCGTCAT	TCCAGCGTGTAGTGTGAAGC
Dkk1	CTCTGCTAGGAGCCAGTGC	CGCACTCCTCATCTTCAGC
Sfrp2	AGGTGTGTGAAGCCTGC	CTTCAGGTCCCTTTCGGAC
Opg	GAACTGCAGTCCGTG AAGC	CAAACTGTGTTTCGCTCTGG
Rankl	TGTACTTTCGAGCGCAGATG	CCCACAATGTGTTGCAGTTC
Tracp	TGAGGACGTGTTCTCTGACC	AAGCGCAAACGGTAGTAAGG
Il1α	GGGTGACAGTATCAGCAACG	TGACAAACTTCTGCCTGACG
Il1β	GGACCCCAAAAGATGAAGG	GTAGCTGCCACAGCTTCTCC
Il6	CGATGATGCACTTGCAGA	CTCTGAAGGACTCTGGCTTTG

Table 1. Sequences of primers (5'→3') used for real time PCR.

40 units of RNase Inhibitor (Invitrogen), 0.1 M of dithiothreitol and 200 units of SuperScript II reverse transcriptase (SSII) (Invitrogen) in a 10 µl final volume of buffer. For each sample, a reaction without SSII was performed and used as negative control. cDNA was then purified using Qiaquick PCR Purification Kit (Qiagen, Courtaboeuf, France) and stored at -20°C.

Real-time PCR

RT-PCR analyses were carried out using a Chromo 4™ (Bio-Rad, Marnes-la-Coquette, France) and SYBR Green detection. Forward and reverse primers were designed using Primer3 software (http://frodo.wi.mit.edu/cgi-bin/primer3/primer3_www.cgi). Studied genes were *Runx2*, Alkaline Phosphatase (*Alp*), *Tgfβ1, Lrp5, Dkk1, Sfrp2, Opg, Rankl, Tracp, Il1α, Il1β, Il6*. Sequences of primers used are given in Table 1. Amplification was done in duplicate in a final volume of 15 µl containing 5 µl of cDNA diluted at 0.2 in sterile distilled water (sample or standard) and 10 µl of iQ SYBR Supermix (Biorad) containing 5 µM of each primer. Then, the following protocol was used: (i) 95°C for 10 min, (ii) amplification and quantification program repeated 40 cycles (95°C for 15 s, 55°C for 11 s, 72°C for 22 s, with a single fluorescence measurement of SYBR green I at each end of cycle), (iii) 65-99°C with a heating rate of 0.1°C and continuous fluorescence measurement. The difference of the expression level was determined by normalization to the expression level of the housekeeping genes (*Hprt1, B2m and Actb*) in parallel runs and quantification was made using a standard curve assay.

Statistical analysis

Statistical analysis was performed with Systat statistical software, release 13 (Systat, San José, CA). All data are expressed as mean±SEM. For each variable, differences between each time point were analyzed by an analysis of variance with the Fisher's least significant difference *post-hoc* test. Data from left and right hindlimb were compared using a paired sample t-test. Differences were considered as significant when $P<0.05$.

Day	Body weight (g)
0	27.9 ± 0.3
7	26.0 ± 0.7
14	26.6 ± 0.5
21	28.1 ± 0.9
28	28.1 ± 0.6

Table 2. Body weight of mice from the BTX groups at day 0 and at the time of sacrifice. Data are provided as mean±SEM.

Results

General findings

24 hours after the BTX injection, all mice showed lameness with hindlimb abduction during tail suspension and toe extension during sitting. Signs of lameness became maximal 48 hours after BTX injection. Body weight did not change significantly from 0 to 28 days despite a non-significant lower weight observed at 7 and 14 weeks (Table 2).

MicroCT analysis

Trabecular bone measurements

3D measurements are summarized in Table 3. In the baseline group, no significant differences were observed between the left and right limb in the baseline group. In the BTX groups, significant differences were observed on the I limb from 7 days and maintained until 21 days. Trabecular bone loss was evidenced (Figure 1) and characterized by lower BV/TV and Tb.N compared to the NI limb (BV/TV at 7 days: -26.5%; 14 days: -31.0%; 21 days: -45.7%). SMI was significantly increased in the I limb from 7 days until 21 days, thus emphasizing an increase in rod-like trabeculae at the expense of plate-like trabeculae. A significant decrease in Tb.Th was observed from 14 days until 28 days; conversely, no significant difference was observed for Tb.Sp. For each time point, significant differences were observed between

		BV/TV (%)	Tb.Th (µm)	Tb.N (1/mm)	Tb.Sp (µm)	SMI
Baseline	Left	17.7±2.0	62±0.2	2.9±0.1	340±3	1.5±0.07
	Right	17.7±0.8	62±0.2	2.9±0.1	320±3	1.6±0.05
7 days	NI	11.7±1.3*	56±0.2*	2.1±0.2*	370±4	1.8±0.08*
	I	8.6±0.6*	52±0.2*	1.7±0.1*	380±4	2.1±0.04*
14 days	NI	11.6±0.9*	59±0.2	1.9±0.1*	390±2	1.8±0.03*
	I	8.0±0.8*	52±0.2*	1.4±0.1*	400±1	2.2±0.03*,†
21 days	NI	11.6±1.1*,†	63±0.1†	1.9±1.9*	440±6	1.9±0.03*
	I	6.3±0.7*,†	52±0.2*	1.2±0.1*,†	480±5*,†	2.2±0.05*,†
28 days	NI	8.7±0.8*,†,‡,§	62±0.2†	1.4±0.1*,†,‡	560±2*,†,‡,§	2.2±0.09*,†,‡,§
	I	6.2±0.4*,†	58±0.1*,†,‡,§	1.1±0.1*,†	580±3*,†,‡,§	2.3±0.06*,†

*NI: left non-immobilized limb, I: right immobilized limb for BTX groups sacrificed at day 7, 14, 21 and 28 days. Baseline: mice sacrificed at day 0 with microCT measurement done on left and right hindlimb. * P<0.05 vs. Baseline, †P<0.05 vs. 7 days, ‡P<0.05 vs. 14 days, §P<0.05 vs. 21 days. The gray boxes indicate a significant difference vs. NI with P<0.05. Data are provided as mean ± SEM.*

Table 3. 3D microCT measurements on trabecular bone.

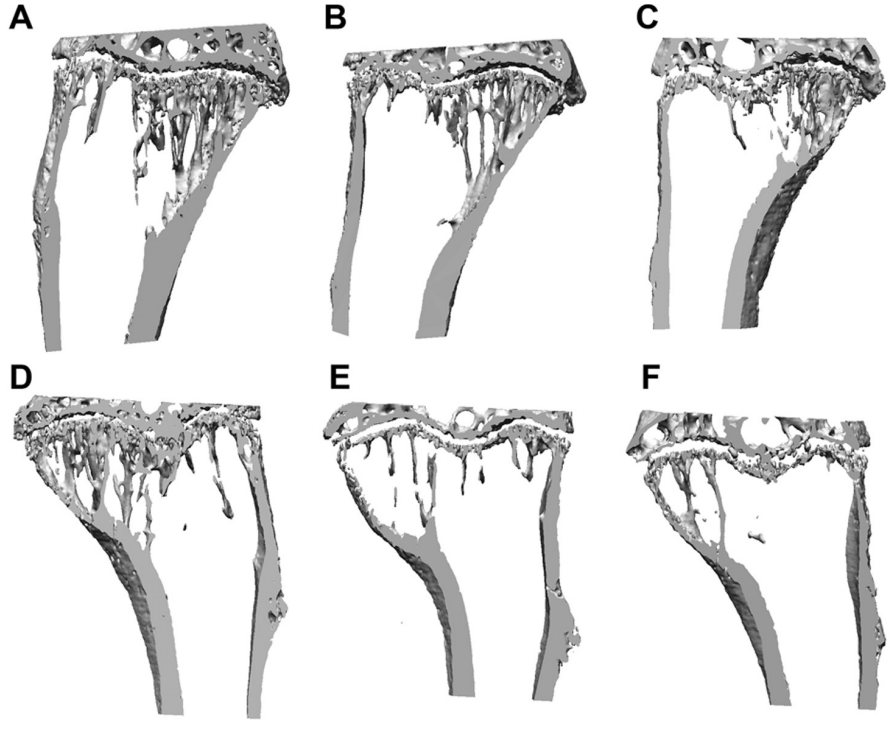

Figure 1. X-ray microCT reconstructions of the left and right hindlimb (**A, D**) at baseline and of the NI left and I right hindlimb at 7 days (**B, E**) and 21 days (**C, F**).

the NI limb and the left limb from the baseline group: BV/TV, Tb.N and Tb.Sp were lower; SMI was higher. Significant increase in Tb.Sp was observed at 28 days in the immobilized and non-immobilized limb compared to baseline animals and the 3 BTX groups sacrificed at 7, 14 and 21 days.

Cortical bone measurements

No significant differences were observed at the diaphysis between I and NI independently of the considered parameter (Table 4). At 28 days, Ct.Ar tended to be lower on the I limb compare to NI limb (P=0.07). When differences were searched be-

		Ct.Th (mm)	Ct.Ar (mm²)	Ps.Ar (mm²)	Es.Ar (mm²)	Porosity (%)
Baseline	Left	0.158±0.006	0.167±0.007	0.274±0.014	0.106±0.007	2.97±0.62
	Right	0.157±0.006	0.145±0.022	0.279±0.014	0.113±0.008	2.32±0.56
7 days	NI	0.150±0.007	0.159±0.005	0.265±0.013	0.105±0.010	1.55±0.43
	I	0.153±0.006	0.161±0.006	0.275±0.019	0.114±0.013	2.78±0.71
14 days	NI	0.144±0.004	0.143±0.007	0.212±0.032	0.086±0.014	2.05±0.67
	I	0.140±0.005	0.107±0.024 †	0.245±0.018	0.077±0.018	3.30±1.04
21 days	NI	0.153±0.008	0.137±0.007 *,†	0.250±0.022	0.114±0.017	2.21±0.77
	I	0.143±0.009	0.134±0.008	0.248±0.018	0.114±0.013	1.38±0.50
28 days	NI	0.151±0.007	0.138±0.005 *,†	0.260±0.015	0.112±0.016	3.01±0.86
	I	0.149±0.005	0.123±0.006	0.243±0.016	0.103±0.011	2.25±0.61

*NI: left non-immobilized limb, I: right immobilized limb for BTX groups sacrificed at day 7, 14, 21 and 28 days. Baseline: mice sacrificed at day 0 with microCT measurement done on left and right hindlimb. * P<0.05 vs. Baseline, †P< 0.05 vs. 7 days. Data are provided as mean±SEM.*

Table 4. 2D microCT measurements on cortical bone.

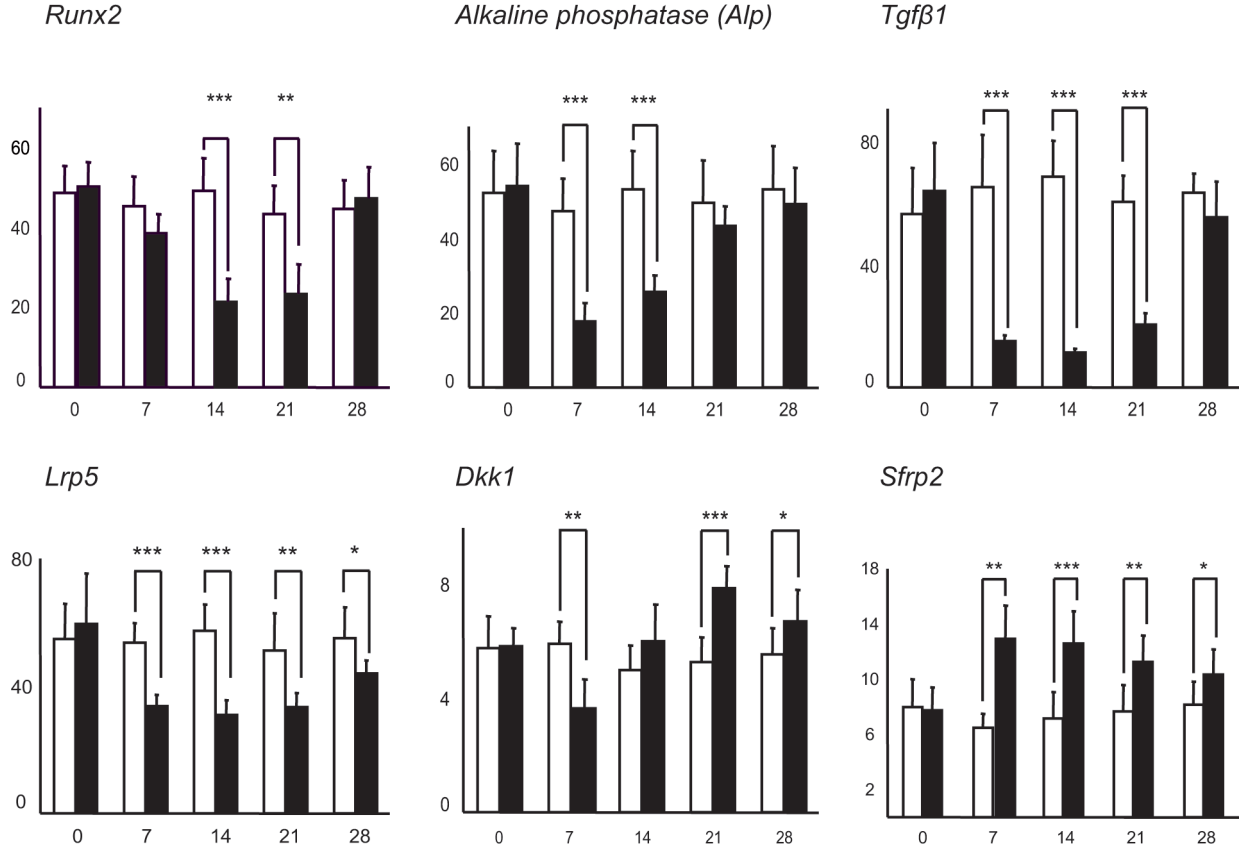

Figure 2. Expression of bone formation markers assessed by qPCR. I limbs for BTX groups (and right side for baseline group) are in black, NI limbs (and left side for baseline group) are in white.

tween each time point, we found a significant decrease of Ct.Ar from the NI limb at 21 and 28 days versus baseline and 7 days.

Gene expression analysis

Quantitative PCR revealed modifications for 11 out of 12 genes analyzed. Results are summarized in Figures 2, 3 and 4. Most of them (10 out of 12) were significantly modified as early as 7 days: *Alp, Tgfβ1, Lrp5, Dkk1, Sfrp2* which are considered as formation indicators and *Rankl, Tracp, Il1α, Il1β* and *Il6* which are considered as resorption indicators. Among the formation markers, gene expression of *Tgfβ1*, a key differentiation factor of osteoblast and gene expression of *Alp*, earlier osteoblast

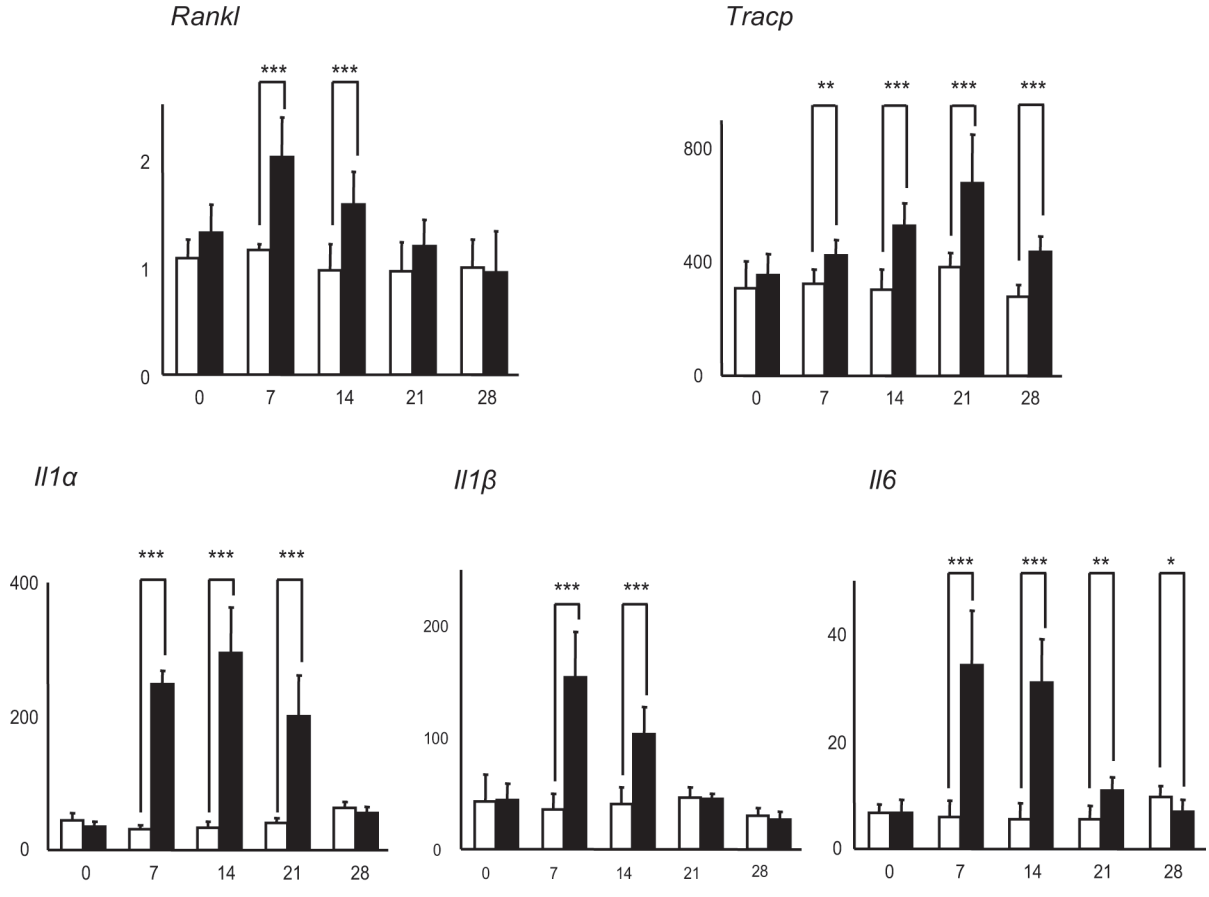

Figure 3. Expression of bone resorption markers assessed by qPCR. I limbs for BTX groups (and right side for baseline group) are in black, NI limbs (and left side for baseline group) are in white.

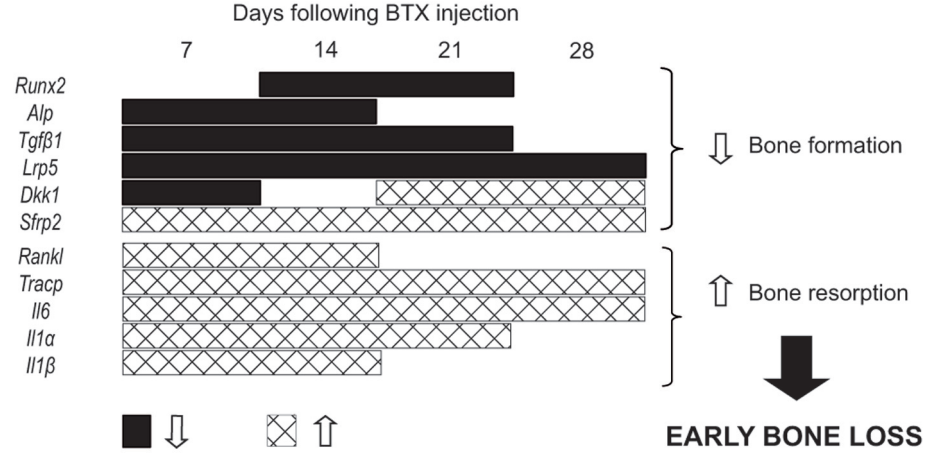

Figure 4. Summary of the kinetic expression of the 11 genes showing a modified expression (*Opg* was not illustrated, because not modified). Black boxes indicate an increase in gene expression, hatched boxes indicate a decrease gene expression.

marker, were significantly decreased in the I limb (Figure 2). The decrease expression was transient as no significant differences were noticed from 14 days for *Alp* and 21 days for *Tgfβ1*. Modification of the *Runx2* transcription factor was delayed; it decreased significantly from 14 until 21 days. Other modifications concerned the Wnt pathway genes. Among them, expression of *Lrp5* was highly depressed from 7 days; such a lower expression was maintained at each time point. Expression of *Sfrp2*, one of the inhibitors of the Wnt pathway, was significantly increased from 7 days and was maintained higher until 28 days. Expression of the second inhibitor of the Wnt pathway, *Dkk1*, was firstly decreased at 7 days and secondarily increased from 21 days until 28 days. All resorption markers were significantly increased as earlier as 7 days (Figure 3). Significant high expression of specific osteoclast marker, *Tracp*, and expression of *Il6* were maintained for each time point. *Rankl* and Il1β expression returned to NI level from 21 days. *Il1α* returned to NI level at 28 days. No significant differences were observed for *Opg*. Figure 4 summarized all results from PCR analysis which explained early trabecular bone loss observed by microCT analysis.

Discussion

Localized paralysis induced by BTX injection in a hindlimb quadriceps results in a rapid and significant trabecular bone loss, trabecular microarchitecture deterioration without cortical modifications in the diaphysis. Major differences between I and NI limb were found at 21 days. These mice had completed their rapid growth phase according the Harlan's normogram. There was no difference in the activity and weight body of the animals meaning that mice did not suffer from the BTX injection as previously found in other studies. Trabecular bone loss was associated with a major modification of local gene expression as earlier as 7 days. These modifications included an increase in bone resorption gene markers (*Rankl, Tracp, Il6, Il1α, Il1β*) and a decrease in bone formation gene markers (*Alp, Tgfβ1, Lrp5*). *Runx2* gene expression was decreased with a delay of 1 week compared to other markers. The gene expression of the two inhibitors of bone formation (*Dkk1* and *Sfrp2*) was increased with a difference in kinetic; gene expression analysis would indicate that *Dkk1* is a late indicator of bone formation compared to *Sfrp2*. Moreover, *Lrp5* was maintained at a low level and *Sfrp2* at a high level all over the time of the study. Our study revealed an early modification of gene expression profile in the bone marrow microenvironment.

In the present study, we have performed a kinetic study in which we showed an early reduction in bone volume from 7 days. Maximal bone loss was found at 21 days, in accordance with previous studies[11]. A profound degradation of bone was observed by microCT, 21 days after BTX injection; a 54.3% reduction in BV/TV was found in the proximal tibia metaphysis. Other recent studies found similar results with a reduction of BV/TV around 40% in 3 weeks in the mouse and 31% in the rat[9,19]. Few kinetic studies have been previously reported but they only presented bone tissue changes obtained by microCT and histomorphometry[10,20]. Bone loss was observed before 21 days and a 25.5% significant decrease in BV/TV was reported as early as 3 days with a very high dose of BTX[20]. Taken together, all these studies including ours, confirm that muscle paralysis due to BTX injection causes a massive and rapid bone loss. Surprisingly, we found no deterioration of cortical bone in the diaphysis between I and NI limb; this result is slightly different from other studies where deteriorations of cortical were found around 3-4 weeks post BTX injection[10,11,20]. In a recent study in the growing rat, we found no effect of BTX on the growth in length of the tibia nor on the mean curvature[21]. These discrepancies could be explained by the use of different strain of mice and also because mice in our study were 5-6 weeks youngers. Our findings permit to understand the pathophysiological mechanisms of bone loss with a removal of trabeculae (as evidenced by a significant Tb.N reduction), indicating an increase in osteoclast activity. Such a mechanism has previously been described by our group in the BTX rat and confirmed by serum TRAcP dosage and osteoclast count of histological sections (after histochemical identification by TRAcP staining)[8]. Similar findings have been confirmed histomorphometrically by others either in the rat or the mouse shown an increase bone resorption associated with a depressed bone formation[8,11,19]. The tendency for Tb.Sp to a non-significant decrease has also been found in a previous kinetic study performed in mice injected with BTX[10]. Interestingly, we found a simultaneous reduction in Tb.Th which appeared later on the I hindlimb. Parfitt has previously shown, in man, that an increase in osteoclast activity is responsible for trabecular perforations and micro-architectural deterioration and these findings have been constitutively reported in postmenopausal osteoporosis[22-24]. On the contrary, osteoporosis with reduction in Tb.Th is due to the reduction in the osteoblastic function (e.g., in glucocorticoid-induced osteoporosis)[25-27]. In our model we evidenced both mechanisms of bone loss leading to severe architectural changes.

Bone remodeling is a physiological complex mechanism that maintains bone mechanically competent by constantly replacing old bone by new bone structure units. It always starts with osteoclastic resorption followed by production of a new bone structure unit by osteoblasts[28,29]. Disuse is associated with an unbalanced bone remodeling caused by an increase in resorption and a decrease in formation[30]. However, most studies are mainly based on histomorphometric data or on serum level bone turnover markers[31]. In the BTX model, we studied for the first time the kinetic evolution of genes involved in bone remodeling. We found an early expression of genes favoring osteoclastogenesis and a simultaneous depression of osteoblastogenesis genes responsible for a rapid bone loss. To our knowledge, only one study reported a molecular analysis of only six genes in a mouse model of disuse caused by immobilization by plaster cast[32]. A marked alteration of both osteoblastic and osteoclastic markers was found as early at 3 days for osteoclastic markers. *Tracp* remained at high level until 21 days of immobilization which is in accordance with our results; other resorption genes had a transient increase like *cathepsin K*. Although we did not assess the expression of this

gene, we also found a transient increase for 3 other resorption genes: *Rankl, Il1α* and *Il1β*. A transient resorption was also reported by measuring TRAcP in the serum of BTX and orchidectomized rats[8]. An increase of *RANK-L* has been observed in osteoblasts obtained from spinal cord injured rats[33]. The effect of the inflammatory cytokines IL1 and IL6 has extensively been investigated since IL6 increases osteoclastogenesis indirectly by upregulating RANKL[34]. Little is known about the influence of disuse on *Il1* or *Il6* expression. In contrast to our results, a decrease in IL6 has been shown in mice submitted to suspension[35].

In the present study, osteoblastic gene markers were altered as early as 7 days except for *Runx2*. Disruption of the *Runx2* gene in mice leads to a complete lack of bone formation and to the inhibition of osteoblast maturation[36]. Thus, the decrease in *Runx2* observed in BTX animals could reflect a decrease in mature osteoblast number. Our findings are in accordance with previous *in vitro* studies showing an inhibition of the osteoblast phenotype associated with a reduction of more than 60% in *Runx2* in cultured cells submitted to low gravity[37]. In contrast, hypergravity strongly increases *Runx2* expression in osteoblast[38]. As mature osteoblasts seem to be decreased due to low *Runx2* expression level, it is not surprising to observe a decrease in *Alp*, a major osteoblastic marker. Similar results were obtained in cells culture under hypogravity[37]. The decrease in these markers was not observed in the spinal cord injury model and remained at a normal level[33]. Transient *Tgfβ* decrease could reflect also a depression of the osteoblastic function. Our results are in accordance with previous studies that observed a role for TGFβ in osteoclast apoptosis and in the recruitment and proliferation of osteoblast precursors cells in the BMU (Basic multicellular unit)[39,40]. A low level of Tgfβ mRNA expression is found in unloaded bones from tail suspension rat model; in contrast, an increase is observed following mechanical loading[41,42]. Among the analyzed bone formation genes, those from the Wnt pathway (*Lrp5* and *Sfrp2*) were maintained altered from 7 days to 28 days. It has been shown that the lack of LRP5 in mice induces an inhibition of osteoblast function associated with a decrease in osteoblast number[43]. Moreover, LRP5 is expressed by cells from the osteoblast lineage; thus, its low expression, associated with an increased expression of *Sfrp*, would reflect an alteration in osteoblastic function. Interestingly, we observed a 2 phases evolution of *Dkk1* including a decrease followed by an increased expression. DKK1 has been extensively studied in different bone disorders where osteoblast function is reduced[14,44]. To our knowledge, only one study reported that the Wnt pathway, including *Lrp5*, is down-regulated in the spinal cord injury model[45]. Although spinal cord injury is not strictly similar to disuse, these results are in accordance with our data. In contrast, Wnt pathway and more specifically *Sclerostin (Sost)* expression have been extensively studied in loading condition; loading inducing a decreased expression of SOST by osteocytes[46-48].

A primary limitation of this study is that we did not have data on SOST expression. In a preliminary study, we could not detect expression of *Sost* and this is easily explained by the fact that SOST is expressed in osteocytes deeply buried inside the bone matrix. Also, no histomorphometric data on osteoclast and osteoblast activities are presented in the present study that would have confirmed qPCR results. However, histomorphometry has been extensively described by our group (and other teams) to characterize the BTX model and this study has focused on the expression of gene that support these findings[8,11]. Another limitation is that we were not able to differentiate genes expressed from hematopoeitic or stromal cells, however it is now known that both types of cells interact and contribute to the microenvironment in contact with mature bone cells.

In conclusion, we have shown the molecular changes implicated in the increased bone resorption and decreased bone formation associated with bone loss due to BTX-induced disuse[30,49]. Both events were rapid and explained the severity of the bone loss since formation and resorption are simultaneously concerned. We showed a strong implication of the Wnt pathway: the inhibitory marker of bone formation sFRP2 appeared more sensible to disuse than DKK1. This study evidenced the need of therapeutic counter-measures that trigger both the increased bone resorption and the decreased bone formation.

Acknowledgements

This work was made possible by grants from the Bioregos2 Contrat Région "Pays de la Loire". Authors thank P. Legras and J. Roux for their help with the animal care (SCAHU) and the technical assistance of the Service Commun de Cytométrie et d'Analyses Nucléotidiques (SCCAN, Angers University) for the qPCR analysis.

References

1. Sievanen H. Immobilization and bone structure in humans. Arch Biochem Biophys 2010;503:146-52.
2. Demulder A, Guns M, Ismail A, Wilmet E, Fondu P, Bergmann P. Increased osteoclast-like cells formation in long-term bone marrow cultures from patients with a spinal cord injury. Calcif Tissue Int 1998;63:396-400.
3. Jee WS, Ma Y. Animal models of immobilization osteopenia. Morphologie 1999;83:25-34.
4. Frost HM. The regional acceleratory phenomenon: a review. Henry Ford Hosp Med J 1983;31:3-9.
5. Chappard D, Chennebault A, Moreau M, Legrand E, Audran M, Basle MF. Texture analysis of X-ray radiographs is a more reliable descriptor of bone loss than mineral content in a rat model of localized disuse induced by the Clostridium botulinum toxin. Bone 2001;28:72-9.
6. Rossetto O, Morbiato L, Caccin P, Rigoni M, Montecucco C. Presynaptic enzymatic neurotoxins. J Neurochem 2006;97:1534-45.
7. Meunier FA, Schiavo G, Molgo J. Botulinum neurotoxins: from paralysis to recovery of functional neuromuscular transmission. J Physiol Paris 2002;96:105-13.
8. Blouin S, Gallois Y, Moreau MF, Baslé MF, Chappard D. Disuse and orchidectomy have additional effects on bone

loss in the aged male rat. Osteoporosis Int 2007;18:85-92.
9. Grimston SK, Goldberg DB, Watkins M, Brodt MD, Silva MJ, Civitelli R. Connexin43 deficiency reduces the sensitivity of cortical bone to the effects of muscle paralysis. J Bone Miner Res 2011;26(9):2151-60.
10. Manske SL, Boyd SK, Zernicke RF. Muscle and bone follow similar temporal patterns of recovery from muscle-induced disuse due to botulinum toxin injection. Bone 2010;46:24-31.
11. Warner SE, Sanford DA, Becker BA, Bain SD, Srinivasan S, Gross TS. Botox induced muscle paralysis rapidly degrades bone. Bone 2006;38:257-64.
12. Ducy P, Zhang R, Geoffroy V, Ridall AL, Karsenty G. Osf2/Cbfa1: a transcriptional activator of osteoblast differentiation. Cell 1997;89:747-54.
13. Hessle L, Johnson KA, Anderson HC, Narisawa S, Sali A, Goding JW, Terkeltaub R, Millan JL. Tissue-nonspecific alkaline phosphatase and plasma cell membrane glycoprotein-1 are central antagonistic regulators of bone mineralization. Proc Natl Acad Sci USA 2002;99:9445-9.
14. Milat F, Ng KW. Is Wnt signalling the final common pathway leading to bone formation? Mol Cell Endocrinol 2009;310:52-62.
15. Gong Y, Slee RB, Fukai N, Rawadi G, Roman-Roman S, Reginato AM, Wang H, Cundy T, Glorieux FH, Lev D and others. LDL receptor-related protein 5 (LRP5) affects bone accrual and eye development. Cell 2001;107:513-23.
16. Lacey DL, Timms E, Tan HL, Kelley MJ, Dunstan CR, Burgess T, Elliott R, Colombero A, Elliott G, Scully S and others. Osteoprotegerin ligand is a cytokine that regulates osteoclast differentiation and activation. Cell 1998;93:165-76.
17. Simonet WS, Lacey DL, Dunstan CR, Kelley M, Chang MS, Luthy R, Nguyen HQ, Wooden S, Bennett L, Boone T and others. Osteoprotegerin: a novel secreted protein involved in the regulation of bone density. Cell 1997;89:309-19.
18. Parfitt AM, Drezner MK, Glorieux FG, Kanis JA, Malluche H, Meunier PJ, Ott SM, Recker RR. Bone histomorphometry: standardization of nomenclature, symbols, and units. Report of the ASBMR Histomorphometry Nomenclature Committee. J Bone Miner Res 1987; 2:595-610.
19. Thomsen JS, Christensen LL, Vegger JB, Nyengaard JR, Bruel A. Loss of bone strength is dependent on skeletal site in disuse osteoporosis in rats. Calcif Tissue Int 2012;90:294-306.
20. Poliachik SL, Bain SD, Threet D, Huber P, Gross TS. Transient muscle paralysis disrupts bone homeostasis by rapid degradation of bone morphology. Bone 2010;46:18-23.
21. Bouvard B, Mabilleau G, Legrand E, Audran M, Chappard D. Micro and macroarchitectural changes at the tibia after botulinum toxin injection in the growing rat. Bone 2012;50:858-64.
22. Parfitt AM, Mathews CH, Villanueva AR, Kleerekoper M, Frame B, Rao DS. Relationships between surface, volume, and thickness of iliac trabecular bone in aging and in osteoporosis. Implications for the microanatomic and cellular mechanisms of bone loss. J Clin Invest 1983; 72:1396-409.
23. Akhter MP, Lappe JM, Davies KM, Recker RR. Transmenopausal changes in the trabecular bone structure. Bone 2007;41:111-6.
24. Kleerekoper M, Villanueva AR, Stanciu J, Sudhaker RD, Parfitt AM. The role of three dimensional trabecular microstructure in the pathogenesis of vertebral compression fractures. Calcif Tissue Int 1985; 37:594-7.
25. Chappard D, Legrand E, Baslé MF, Fromont P, Racineux JL, Rebel A, Audran M. Altered trabecular architecture induced by corticosteroids: a bone histomorphometric study. J Bone Miner Res 1996;11:676-85.
26. Dalle Carbonare L, Arlot ME, Chavassieux PM, Roux JP, Portero NR, Meunier PJ. Comparison of trabecular bone microarchitecture and remodeling in glucocorticoid-induced and postmenopausal osteoporosis. J Bone Miner Res 2001;16:97-103.
27. Dempster DW, Arlot MA, Meunier PJ. Mean wall thickness and formation periods of trabecular bone packets in corticosteroid-induced osteoporosis. Calcif Tissue Int 1983;35:410-7.
28. Frost HM. Some ABCs of skeletal pathophysiology. III: Bone balance and the delta B.BMU. Calcif Tissue Int 1989;45:131-3.
29. Parfitt AM. The mechanism of coupling: a role for the vasculature. Bone 2000;26:319-23.
30. Takata S, Yasui N. Disuse osteoporosis. J Med Invest 2001;48:147-56.
31. Lueken SA, Arnaud SB, Taylor AK, Baylink DJ. Changes in markers of bone formation and resorption in a bed rest model of weightlessness. J Bone Miner Res 1993;8:1433-8.
32. Rantakokko J, Uusitalo H, Jamsa T, Tuukkanen J, Aro HT, Vuorio E. Expression profiles of mRNAs for osteoblast and osteoclast proteins as indicators of bone loss in mouse immobilization osteopenia model. J Bone Miner Res 1999;14:1934-42.
33. Jiang SD, Jiang LS, Dai LY. Effects of spinal cord injury on osteoblastogenesis, osteoclastogenesis and gene expression profiling in osteoblasts in young rats. Osteoporosis Int 2007;18:339-49.
34. Schett G. Effects of inflammatory and anti-inflammatory cytokines on the bone. Eur J Clin Invest 2011;41:1361-6.
35. Armstrong JW, Balch S, Chapes SK. Interleukin-2 therapy reverses some immunosuppressive effects of skeletal unloading. J Appl Physiol 1994;77:584-9.
36. Komori T, Yagi H, Nomura S, Yamaguchi A, Sasaki K, Deguchi K, Shimizu Y, Bronson RT, Gao YH, Inada M and others. Targeted disruption of Cbfa1 results in a complete lack of bone formation owing to maturational arrest of osteoblasts. Cell 1997;89:755-64.
37. Ontiveros C, McCabe LR. Simulated microgravity suppresses osteoblast phenotype, Runx2 levels and AP-1 transactivation. J Cell Biochem 2003;88:427-37.

38. Morita S, Nakamura H, Kumei Y, Shimokawa H, Ohya K, Shinomiya K. Hypergravity stimulates osteoblast phenotype expression: a therapeutic hint for disuse bone atrophy. Ann N Y Acad Sci 2004;1030:158-61.
39. Hughes DE, Dai A, Tiffee JC, Li HH, Mundy GR, Boyce BF. Estrogen promotes apoptosis of murine osteoclasts mediated by TGF-beta. Nat Med 1996;2:1132-6.
40. Pfeilschifter J, Wolf O, Naumann A, Minne HW, Mundy GR, Ziegler R. Chemotactic response of osteoblastlike cells to transforming growth factor? J Bone Miner Res 1990;5:825-30.
41. Zhang R, Supowit SC, Hou X, Simmons DJ. Transforming growth factor-beta2 mRNA level in unloaded bone analyzed by quantitative *in situ* hybridization. Calcif Tissue Int 1999;64:522-526.
42. Raab-Cullen DM, Thiede MA, Petersen DN, Kimmel DB, Recker RR. Mechanical loading stimulates rapid changes in periosteal gene expression. Calcif Tissue Int 1994;55:473-8.
43. Kato M, Patel MS, Levasseur R, Lobov I, Chang BH, Glass DA 2nd, Hartmann C, Li L, Hwang TH, Brayton CF and others. Cbfa1-independent decrease in osteoblast proliferation, osteopenia, and persistent embryonic eye vascularization in mice deficient in Lrp5, a Wnt coreceptor. The Journal of Cell Biology 2002;157:303-14.
44. Oshima T, Abe M, Asano J, Hara T, Kitazoe K, Sekimoto E, Tanaka Y, Shibata H, Hashimoto T, Ozaki S and others. Myeloma cells suppress bone formation by secreting a soluble Wnt inhibitor, sFRP-2. Blood 2005;106:3160-5.
45. Jiang SD, Yan J, Jiang LS, Dai LY. Down-regulation of the Wnt, estrogen receptor, insulin-like growth factor-I, and bone morphogenetic protein pathways in osteoblasts from rats with chronic spinal cord injury. Joint Bone Spine 2011;78:488-92.
46. Robling AG, Niziolek PJ, Baldridge LA, Condon KW, Allen MR, Alam I, Mantila SM, Gluhak-Heinrich J, Bellido TM, Harris SE and others. Mechanical stimulation of bone in vivo reduces osteocyte expression of Sost/sclerostin. The Journal of Biological Chemistry 2008; 283:5866-5875.
47. Robling AG, Kedlaya R, Ellis SN, Childress PJ, Bidwell JP, Bellido T, Turner CH. Anabolic and catabolic regimens of human parathyroid hormone 1-34 elicit bone- and envelope-specific attenuation of skeletal effects in Sost-deficient mice. Endocrinology 2011;152:2963-75.
48. Tu X, Rhee Y, Condon KW, Bivi N, Allen MR, Dwyer D, Stolina M, Turner CH, Robling AG, Plotkin LI and others. Sost downregulation and local Wnt signaling are required for the osteogenic response to mechanical loading. Bone 2012;50:209-17.
49. Dehority W, Halloran BP, Bikle DD, Curren T, Kostenuik PJ, Wronski TJ, Shen Y, Rabkin B, Bouraoui A, Morey-Holton E. Bone and hormonal changes induced by skeletal unloading in the mature male rat. Am J Physiol 1999;276:E62-9.